The FASEB Journal article fj.201701267R. Published online December 22, 2017.

THE FASEB JOURNAL • RESEARCH • www.fasebj.org

Alternative routes for synthesis of *N*-linked glycans by Alg2 mannosyltransferase

Sheng-Tao Li,* Ning Wang,* Xin-Xin Xu,* Morihisa Fujita,* Hideki Nakanishi,* Toshihiko Kitajima,* Neta Dean,[†,1] and Xiao-Dong Gao[*,2]

*Key Laboratory of Carbohydrate Chemistry and Biotechnology, Ministry of Education, School of Biotechnology, Jiangnan University, Wuxi, China; and [†]Department of Biochemistry and Cell Biology, Stony Brook University, Stony Brook, New York, USA

ABSTRACT: Asparagine (*N*)-linked glycosylation requires the ordered, stepwise synthesis of lipid-linked oligosaccharide (LLO) precursor $Glc_3Man_9GlcNAc_2$–pyrophosphate–dolichol ($Glc_3Man_9Gn_2$-PDol) on the endoplasmic reticulum. The fourth and fifth step of LLO synthesis are catalyzed by Alg2, an unusual mannosyltransferase (MTase) with two different MTase activities; Alg2 adds both an α1,3- and α1,6-mannose onto $ManGlcNAc_2$-PDol to form the trimannosyl core $Man_3GlcNAc_2$-PDol. The biochemical properties of Alg2 are controversial and remain undefined. In this study, a liquid chromatography/mass spectrometry-based quantitative assay was established and used to analyze the MTase activities of purified yeast Alg2. Alg2-dependent $Man_3GlcNAc_2$-PDol production relied on net-neutral lipids with a propensity to form bilayers. We further showed addition of the α1,3- and α1,6-mannose can occur independently in either order but at differing rates. The conserved C-terminal EX_7E motif, *N*-terminal cytosolic tail, and 3 G-rich loop motifs in Alg2 play crucial roles for these activities, both *in vitro* and *in vivo*. These findings provide insight into the unique bifunctionality of Alg2 during LLO synthesis and lead to a new model in which alternative, independent routes exist for Alg2 catalysis of the trimannosyl core oligosaccharide.—Li, S.-T., Wang, N., Xu, X.-X., Fujita, M., Nakanishi, H., Kitajima, T., Dean, N., Gao, X.-D. Alternative routes for synthesis of *N*-linked glycans by Alg2 mannosyltransferase. FASEB J. 32, 000–000 (2018). www.fasebj.org

KEY WORDS: *N*-glycosylation · lipid-linked oligosaccharide · LC-MS

In eukaryotes, *N*-glycosylation starts with assembly of a lipid-linked oligosaccharide (LLO) precursor, $Glc_3Man_9GlcNAc_2$–pyrophosphate–dolichol ($Glc_3Man_9Gn_2$-PDol), on the endoplasmic reticulum membrane (1–3). Addition of the 14 LLO sugars is carried out sequentially by 12 different asparagine-linked glycosylation (Alg) glycosyltransferases (GTase) (4–6). Extensive effort in the past three decades has led to the identification all the *ALG* genes required for LLO biosynthesis. The biochemistry of all the Alg GTases is also well characterized, with the exception of Alg2. Alg2 catalyzes addition of both the α-1,3- and α-1,6-linked mannose (Man) onto Man_1Gn_2-PDol to form the trimannosyl core Man_3Gn_2-PDol.

The molecular details of Alg2 have been a long-standing controversial issue, in part because it is an unusual GTase that catalyzes two different enzymatic reactions whose order has not been resolved. Earlier phenotypic analyses of yeast, fungal, and human *alg2* mutants suggested Alg2 is required to elongate either Man_1Gn_2-PDol to Man_2Gn_2-PDol or Man_2Gn_2-PDol to Man_3Gn_2-PDol (5, 7–10). Both these reactions are catalyzed by Alg2 because recombinant Alg2 can elongate Man_1Gn_2-PDol substrate to produce Man_3Gn_2-PDol *via* a Man_2Gn_2-PDol intermediate (11). Similarly, Alg2 immunoprecipitated from extracts of yeast microsomal membranes also displays both α1,3- and α1,6-mannosyltransferase (MTase) activities (12). Because both *in vitro* and *in vivo* studies identified Man-(α1-3)-Man-Gn_2-PDol as the only tetrasaccharide intermediate of the Alg2 reaction, the current accepted model for the order of Man addition by Alg2 is α1,3-mannosylation followed by α1,6-mannosylation to yield the branched core pentasaccharide product Man-(α1,3)[Man-(α1,6)]-Man_1Gn_2-PDol.

A problem with this model is it contradicts experiments conducted almost 40 yr ago that suggested the Man_2Gn_2-PDol tetrasaccharide intermediate is a mixture

ABBREVIATIONS: 3HA, three *N*-terminal hemagglutinin in repeats; Alg, asparagine-linked glycosylation; CL, cardiolipin; DGDG, digalactosyldiglyceride; ESI-MS, electrospray ionization mass spectrometry; 5-FOA, 5-fluoroorotic acid; GDP, guanosine 5′-diphosphate; Gn_2, $GlcNAc_2$; GTase, glycosyltransferase; HA, hemagglutinin; IPTG, isopropyl-β-D-thiogalactopyranoside; LC-MS, liquid chromatography/mass spectrometry; LLO, lipid-linked oligosaccharide; Man, mannose; MTase, mannosyltransferase; PC, phosphatidylcholine; PDol, pyrophosphate–dolichol; PE, phosphatidylethanolamine; PPhy, pyrophosphate–phytanyl; PS, phosphatidylserine; Trx, thioredoxin; UPLC, ultraperformance liquid chromatography; WT, wild type

[1] Correspondence: Stony Brook University, Stony Brook, New York, USA. E-mail: neta.dean@stonybrook.edu

[2] Correspondence: Jiangnan University, 1800 Lihu Avenue, Wuxi 214122, China. E-mail: xdgao@jiangnan.edu.cn

doi: 10.1096/fj.201701267R

This article includes supplemental data. Please visit *http://www.fasebj.org* to obtain this information.

of the Man-(α1-3)-Man-Gn_2-PDol and Man-(α1-6)-Man-Gn_2-PDol isomers. These earlier experiments showed that Man_2Gn_2-PDol isolated from yeast microsomes incubated with uridine diphosphate *N*-acetylglucosamine–GlcNAc and guanosine 5′-diphosphate (GDP)-[^{14}C] Man contains about 85% Man-(α1-3)-Man-Gn_2 and 15% Man-(α1-6)-Man-Gn_2 (13). In addition, two isomeric tetrasaccharide Man_2Gn_2-PDol intermediates, Man-(α1-3)-Man-Gn_2-PDol and Man-(α1-6)-Man-Gn_2-PDol, accumulate in yeast *alg2* mutants (8). These results imply that Alg2 can directly transfer the α1-6–linked Man to Man_1Gn_2-PDol. However, direct evidence for α1,6-mannosylation on Man_1Gn_2-PDol by purified Alg2 protein is lacking.

In addition to the order of the Alg2-mediated reactions, there are also conflicts in the literature regarding how Alg2 structure relates to its function. For instance, Alg2 contains a highly conserved EX_7E motif, which is the signature sequence of CaZY families 3, 4, and 5 retaining GTases (14). Several groups have investigated the biologic importance of the EX_7E motif in enzyme activity of Alg2 but reported contradictory results (11, 12).

Here we make use of a novel liquid chromatography/mass spectrometry (LC-MS)-based Alg2 assay to help clarify the discrepancies that currently exist. We previously established an LC-MS–based quantitative assay for the Alg1 β1,4-MTase whose catalytic step precedes Alg2. In that assay, recombinant Alg1 generates Man-(β1,4)-Gn_2-PPhy from a GlcNAc-(β1,4)-GlcNAc-pyrophosphate–phytanyl (PPhy):Gn_2-PPhy acceptor substrate (15). Here, we coupled this approach to develop a quantitative *in vitro* assay for Alg2, using the Alg1-generated Man_1Gn_2-PPhy product as the acceptor for purified Alg2. Analysis of Alg2 activity confirmed its dual α1,3- and 1,6-Alg2 MTase activities, which required the presence of lipids. This assay also permitted the successful separation and characterization of the tetrasaccharide intermediates of the Alg2 reaction, including both Man-(α1-6)-Man-Gn_2 and Man-(α1-3)-Man-Gn_2 LLOs. By combining mutational analyses of Alg2 *in vitro* and *in vivo*, we established an essential role of the EX_7E putative catalytic motif, as well as 3 highly conserved G-rich loops, and the *N*-terminal cytosolic tail. These data lead to the proposal of a new model for LLO synthesis, in which the fourth and fifth steps can occur independently.

MATERIALS AND METHODS

Plasmid construction

To construct the *Escherichia coli* expression plasmid pET32-scAlg2, *scALG2* was amplified from genomic *Saccharomyces cerevisiae* (sc) DNA and inserted into the pET32 *Bam*HI and *Xho*I sites in frame with an *N*-terminal thioredoxin (Trx)-His_6-tag (Thermo Fisher Scientific, Waltham, MA, USA). To construct the yeast expression plasmid pRS316-TEF-scALG2, the *TEF1* promoter sequence (position −1 to −500 upstream of *TEF1*) was cloned into the *Sac*I and *Spe*I sites of pRS316, an integrative *CEN6/URA3* vector to generate pRS316-TEF. The *scALG2* open reading frame was then inserted downstream the *TEF1* promoter as a *Spe*I and *EcoR*I fragment. To express *scALG2* under its own promoter, 1 kB of *ALG2* upstream sequence (position −1 to −1000 upstream of *ALG2*) was cloned in the *Sac*I and *Spe*I sites of the *CEN6/TRP1* integrative plasmid pRS314 to generate pRS314-ALG2pr. A *Spe*I/*Xho*I fragment containing the *scALG2* open reading frame with 3 *N*-terminal hemagglutinin in repeats (3HA) was constructed by PCR and cloned into pRS314-ALG2pr. This generated pRS314-3HA-scALG2, in which *scALG2* expression is driven by its own promoter. To generate a series of plasmids that expresses various *alg2* mutant alleles as shown in figures 4–7, pRS314-3HA-ALG2 was subjected to mutagenesis by overlapping PCR (16). All mutations and PCR-generated fragments were confirmed by DNA sequence analysis (BGI, Shenzhen, China). Sequences of primers used in this study are available upon request.

Expression and purification of recombinant Alg2 proteins

To purify recombinant yeast scAlg2 protein, pET32-scAlg2 was transformed into *E. coli* DE3 cells (Thermo Fisher Scientific), and positive clones were selected by ampicillin (100 μg/ml) and chloramphenicol (34 μg/ml) resistance. Single colonies were cultured in Terrific-Broth (1.2% tryptone, 2.4% yeast extract, 0.5% glycerol, 17 mM KH_2PO_4 and 72 mM K_2HPO_4) at 37°C until the OD_{600} value reached 1.0. Cultures were cooled to 16°C and induced with 0.1 mM isopropyl-β-D-thiogalactopyranoside (IPTG; Sangon Biotech, Shanghai, China). After ~12 h, cells were collected, resuspended in buffer A [25 mM Tris-HCl (pH 8.0); 150 mM NaCl], and disrupted by sonication on ice. After centrifugation to remove cellular debris (4000*g*, 20 min, 4°C), membranes in the lysate were pelleted by centrifugation (20,000*g*, 90 min, 4°C). Proteins in the membrane fraction were solubilized for 1 h in buffer A containing 1% Triton X-100. His-Alg2 was purified from the detergent-soluble membrane fraction by binding to a HisTrap HP affinity column (GE Healthcare Life Sciences, Little Chalfont, UK). Bound His-Alg2 was eluted with buffer A containing 0.5% Triton X-100 and 500 mM imidazole, dialyzed against buffer B [25 mM Tris-HCl (pH 8.0), 50 mM NaCl, 0.5% Triton X-100], and concentrated with Amicon Ultra 10K NMWL filter units (EMD Millipore, Billerica, MA, USA). Protein concentration was determined by the bicinchoninic acid assay (Sangon Biotech). Proteins from each step of purification were separated by 12% SDS-PAGE gel, followed by staining with Coomassie Brilliant Blue R-250.

Preparation of *E. coli* membrane and proteoliposomes

Bacterial membrane fractions used for *in vitro* Alg2 MTase assays were prepared from *E. coli* (DE3) harboring the empty plasmid pET32. Overnight cultures (10 ml) were disrupted by sonication in buffer A, followed by centrifugation (4000*g*, 20 min, 4°C) to remove cellular debris. Membranes were pelleted from the lysate by centrifugation at 100,000*g* for 60 min at 4°C. After homogenization in 50 μl of [50 mM Tris–acetate (pH 8.5); 30% glycerol], membranes were heated at 100°C for 3 min to inactivate endogenous proteins.

Proteoliposomes were prepared as described (17). Briefly, commercially available lipids, including digalactosyldiglyceride (DGDG; Sigma-Aldrich, St. Louis, MO, USA), cardiolipin (CL; Sigma-Aldrich), phosphatidylserine (PS; Sigma-Aldrich), phosphatidylcholine (PC; Sinophara Chemical Reagent, Shanghai, China), and phosphatidylethanolamine (PE; Sinophara Chemical Reagent) were dissolved in chloroform–methanol (9:1, v/v). To obtain a thin layer of dry lipids, the solvent was removed under a nitrogen gas stream and high vacuum. Dry lipids were homogenized in 50 mM Tris–acetate (pH 8.5), and the resulting liposomes were mixed with purified recombinant Alg2 protein to a final concentration of 100 mg/ml lipid and 0.9 mg/ml protein.

Measurement of *in vitro* Alg2 MTase activity

The acceptor phytanyl oligosaccharide, Man-(β1,4)-Gn-(β1,4)-Gn-PP-phytanyl (Man_1Gn_2-PPhy), was synthesized from Gn-(β1,4)-Gn-PP-phytanyl (Gn_2-PPhy) using yeast Alg1 as described (15). The standard Alg2 assay reaction mixture contained 14 mM 2-(*N*-morpholino)ethanesulfonic acid (pH 6.0), 4 mM potassium citrate, 10 mM $MgCl_2$, 0.05% NP-40, 50 μM Man_1Gn_2-PPhy, 2 mM GDP-Man (Sigma-Aldrich), 1 M sucrose, 10 μl of *E. coli* membrane, and 2 μM purified Alg2 in a total volume of 60 μl. To measure Alg2 *in vitro* activity as a function of lipid, instead of *E. coli* membranes, proteoliposomes were prepared as described above. Ten microliters of proteoliposomes was assayed using otherwise identical reaction conditions, incubated at 30°C for 10 h, and heated at 100°C for 3 min to inactivate Alg2 enzymatic activity.

Reaction products were analyzed as follows: 20 mM hydrogen chloride (0.2 ml) was added to the reaction to hydrolyze glycan-PP-phytanyl. After 1 h incubation at 100°C, the water-soluble glycan-containing fraction was desalted by solid-phase extraction using 1 ml Supelclean ENVI-Carb Slurry (Sigma-Aldrich) and lyophilized. Dried samples were dissolved in water before ultraperformance liquid chromatography (UPLC)-electrospray ionization–mass spectrometry (ESI-MS) analysis. Samples were analyzed on a TSQ Quantum Ultra (Thermo Fisher Scientific) coupled to a Dionex Ultimate 3000 UPLC system (Thermo Fisher Scientific). Glycans were applied to an Acquity UPLC BEH Amide column (1.7 μm, 2.1 × 100 mm; Waters, Beverly, MA, USA) and eluted with an acetonitrile gradient with a flow rate 0.2 ml/min. The gradient program was set as follows: 0 to 2 min, isocratic 80% acetonitrile; 2 to 15 min, 80 to 50% acetonitrile; 15 to 18 min, isocratic 50% acetonitrile. Eluent was monitored by measuring total ions at positive mode in the mass range of *m/z* 400 to 1000. The relative percentage of oligosaccharides was calculated according their peak intensity in LC-ESI-MS by Xcalibur 2.0 (Thermo Fisher Scientific).

Mannosidase digestions

Digestions of glycans (2.5 nM) with 3.2 U of α1,2-3-mannosidase (*Xanthomonas manihotis*; New England Biolabs, Ipswich, MA, USA), 4 U of α1,6-mannosidase (*X. manihotis*; New England Biolabs), and 0.1 mU of α1,2-mannosidase (*Aspergillus saitoi*; ProZyme, Hayward, CA, USA) were performed in 10 μl with buffers supplied by the manufacturer at 25°C for 16 h.

Yeast growth, strain construction, and plasmid shuffling

S. cerevisiae W303a (MAT a*his3-11 leu2-3, 112 ura3-1 trp1-1 ade2-1 can1-100*) was used as the parental strain in this study. Standard yeast genetic methods and media were used for the construction and growth of yeast strains (18). YPAD contained 1% yeast extract, 2% peptone A, 50 mg/L adenine sulfate, and 2% glucose. Synthetic dextrose contained 6.7 g/L yeast nitrogen base, 2 g/L amino acid mix without appropriate selectable supplements, and 2% glucose. For solid media, agar was added to 2%.

LST1 (W303a plus *TEFpr-scALG2::URA3*) contains plasmid-borne *S. cerevisiae ALG2* whose expression is driven by the *TEF1* promoter. LST1 was constructed by introducing the *URA3*-marked plasmid pRS316-TEF-scALG2 into W303a. Chromosomal *ALG2* was then replaced with *His3MX6* by PCR-mediated recombination to generate LST2 (LST1 plus *alg2Δ::His3MX6*) (19). LST2 was transformed with a series of *TRP1*-marked plasmids (pRS314-3HA-scALG2), which express 3HA-tagged *scALG2* wild type (WT) or *alg2* mutant alleles under the control of the *ALG2* promoter. Transformants (single colonies) were cultured in YPAD, followed by spotting on synthetic dextrose media lacking tryptophan and spotting on the same media containing 0.1% 5-fluoroorotic acid (5-FOA) to select for *TRP1*-marked plasmid-borne *ALG2* alleles and against the *URA3*-marked plasmid-borne *ALG2*.

Membrane protein isolation and Western blot analysis

Membrane proteins were extracted from yeast as described (20). Briefly, exponentially growing yeast cells (5 OD_{600} units) were collected and resuspended in 500 μl S-buffer (1 M sorbitol, 2 mM $MgCl_2$, 0.14% β-mercaptoethanol, 50 mM Tris-HCl, pH 7.5) containing 10 U lyticase (Sigma-Aldrich). After incubation at 30°C for 30 min, spheroplasts were pelleted (9000*g*, 1 min, 4°C) and washed twice with ice-cold S-buffer. The spheroplast pellet was lysed in 400 μl ice-cold lysis buffer [0.2 M sorbitol, 1 mM EDTA, 50 mM Tris-HCl (pH 7.5), 1 mM PMSF] by 10 cycles of vortexing with glass beads (425–600 μm; Sigma-Aldrich) for 1 min and incubation on ice for 1 min. Cell debris was removed by low-speed centrifugation (3000*g*, 10 min, 4°C), and the supernatant was centrifuged at 100,000*g* for 30 min at 4°C. The resulting pellet was used as membrane fraction. After solubilization with lysis buffer containing 1% Triton X-100, protein concentration in these membrane fractions was determined by the bicinchoninic acid assay.

For Western blot analysis, 10 μg of protein was separated by 12% SDS-PAGE, followed by transfer onto PVDF (Bio-Rad, Hercules, CA, USA) membrane. The membrane was incubated with anti-hemagglutinin (HA) mouse antibody (TransGen Biotech, Beijing, China), washed, and incubated with anti-mouse IgG–horseradish peroxidase (TransGen Biotech). Immunoreactive bands were visualized by ECL (Bio-Rad).

RESULTS

New LC-MS–based quantitative assay confirms dual MTase activities of purified yeast Alg2

To develop an LC-MS–based assay to measure Alg2 enzyme activity, we first purified recombinant Alg2 protein from *E. coli*. Yeast *ALG2* with an *N*-terminal Trx tag (11) was overexpressed in *E. coli* and purified from the membrane fraction as described in Materials and Methods. SDS-PAGE analysis of the purified protein revealed a single band of about 68 kDa, corresponding to Trx-scAlg2 (**Fig. 1*A***).

To produce the Alg2 LLO acceptor analog Man-(β1,4)-Gn_2-PPhy, we used a chemoenzymatic approach (see Materials and Methods) (15). This Man-(β1,4)-Gn_2-PPhy acceptor was incubated with purified recombinant Trx-scAlg2 for 10 h at 30°C. After chemical release from phytanyl, the glycan products were analyzed by UPLC-ESI-MS. To enhance sensitivity and avoid the ionization reduction of oligosaccharides by salt from UPLC eluent (21), we used only water and acetonitrile in the mobile phase, as this results in a stronger oligosaccharide signal in positive-mode ESI-MS. This procedure purportedly separates the released glycan into α- and β-anomeric forms of oligosaccharides (Fig. 1*B*) (15). Indeed, ESI-MS spectrum of these peaks gave a single molecular mass at *m/z* 609, corresponding to $[Gn_2\text{-M} + Na]^+$ (Fig. 1*C*).

Using a standard reaction mixture containing purified scAlg2, LLO acceptor, and GDP-Man, scAlg2 activity was

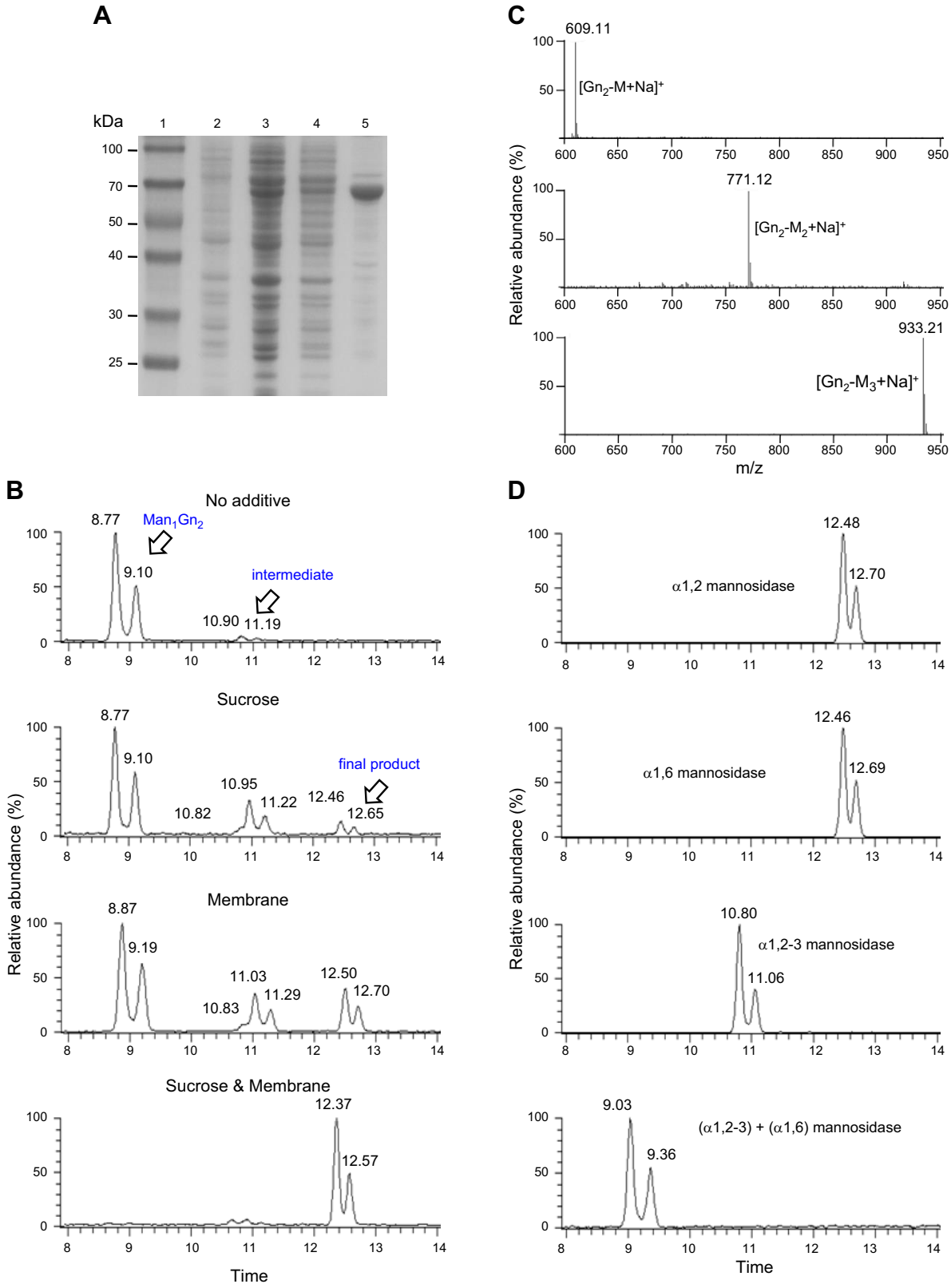

Figure 1. LC-MS–based Alg2 MTase assay. *A*) SDS-PAGE of Trx-scAlg2. Lane 1, molecular markers; lane 2, *E. coli* lysate before IPTG induction; lane 3, *E. coli* lysate after induction with 0.1 mM IPTG; lane 4, membrane fraction solubilized with 1% Triton X-100; lane 5, purified Trx-scAlg2. *B*) Effect of sucrose and membrane on Trx-scAlg2 MTase activity. Reactions were performed using purified Trx-scAlg2, GDP-Man, and chemoenzymatically synthesized acceptor substrate (Man_1Gn_2-PPhy) in basal buffer without any additives (no additive), with 1 M sucrose (sucrose), heat-inactivated *E. coli* membrane (membrane), or 1 M sucrose and heat-inactivated *E. coli* membrane (sucrose and membrane). After incubation at 30°C for 10 h, glycans released from phytanyl oligosaccharides were subjected to LC-MS analysis. Positions of Man_1Gn_2 as well as intermediate and predicted final

(*continued on next page*)

TABLE 1. *Relative percentage of oligosaccharide produced by Alg2 as a function of reaction conditions*[a]

Reaction buffer	Man_1-Gn_2 (%)	Man_2-Gn_2 (%)	Man_3-Gn_2 (%)
No additive	96%	4%	0
Sucrose	67%	25%	8%
Membrane	53%	25%	22%
Sucrose and membrane	0	5%	95%

Reactions were performed using purified Trx-scAlg2, GDP-Man, and Man_1Gn_2-PPhy in 14 mM 2-(*N*-morpholino)ethanesulfonic acid (pH 6.0), 4 mM potassium citrate, 10 mM $MgCl_2$, 0.05% NP-40. After mixing, 1 M sucrose (sucrose), heat-inactivated *E. coli* membrane (membrane), or 1 M sucrose and membrane (sucrose and membrane) was added and reactions incubated at 30°C for 10 h. Oligosaccharides released from various LLOs in mixture were analyzed by LC-MS. [a]Relative percentage of oligosaccharide was calculated by dividing area of each corresponding oligosaccharide peak to total area of all peaks. Chromatograms of oligosaccharides in each of these reactions are shown in Fig. 1*B*.

barely detected (Fig. 1*B*, no additive). Under these conditions, small amounts of intermediate oligosaccharides (peaks around 11.0 min) were detected but no final product. In contrast, addition of 1 M sucrose to the reaction mixture enhanced the MTase activities; increased oligosaccharide products of both intermediate (peaks around 11.0 min) and the final product (peaks around 12.5 min) were observed (Fig. 1*B*, sucrose). Addition of membranes prepared from *E. coli* that did not express Alg2 resulted in a further stimulation of Alg2 activity (Fig. 1*B*, membrane). The simultaneous addition of sucrose and membranes resulted in almost the complete conversion of the substrate, Man_1-Gn_2 (peaks around 9.0 min), to the predicted final product oligosaccharide (peaks around 12.5 min) (Fig. 1*B*, sucrose and membrane). As shown in Fig. 1*C*, ESI-MS analyses of elutes around 11.0 min and around 12.5 min gave peaks at *m/z* 771 and *m/z* 933, corresponding to $[Gn_2\text{-}M_2 + Na]^+$ and $[Gn_2\text{-}M_3 + Na]^+$, respectively. These results demonstrated that recombinant scAlg2 attached 2 Man residues to Man_1Gn_2-PP.

To determine the structure of these oligosaccharides, the reaction product around 12.5 min was collected, digested with linkage-specific mannosidases, and again analyzed by ESI-MS (Fig. 1*D*). This experiment demonstrated that the Alg2 reaction products were resistant to both α1,2-mannosidase and α1,6-mannosidase, but were sensitive to α1,6-mannosidase after treatment with α1,2-3-mannosidase (Fig. 1*D*). Because the α1,6-mannosidase used in this experiment can only hydrolyze a terminal α1,6-Man linked to a nonbranched sugar, we inferred that recombinant scAlg2 transferred 2 Man residues to the β1,4-Man of the Man_1Gn_2-PPhy substrate with α1,6 and α1,3-linkages, yielding Man-(α1,3)[Man-(α1,6)]-Man_1Gn_2-PPhy. These two different Alg2-dependent activities are consistent with previous experiments that demonstrated its bifunctionality (11, 12).

To quantitate each of the Alg2 MTase activities more carefully, the relative percentage of oligosaccharides remaining after completion of the reactions performed in Fig. 1*B* was determined. As shown in **Table 1**, after a 10 h reaction, 95% of the Man_1Gn_2 substrate was fully converted to the final Man_3Gn_2 product when both 1 M sucrose and membranes were present (Fig. 1*B*, sucrose and membrane). Without these additives, only 4% of substrate was converted into intermediate (Fig. 1*B*, no additive). Furthermore, reactions supplemented with either 1 M sucrose or *E. coli* membranes produced the same amount (25%) of intermediate Man_2Gn_2 but different amounts of remaining Man_1Gn_2 substrate and final product (Table 1). Addition of *E. coli* membranes resulted in 22% more final Man_3Gn_2 product and 53% less remaining substrate, demonstrating a more robust MTase activity under these conditions (Fig. 1*B*, cf. sucrose and membrane). These results also underscore that this assay is sufficiently sensitive to quantitatively distinguish differences in each of the 2 Alg2 MTase activities.

MTase activity of Trx-scAlg2 relies on net neutral-bilayer lipids

We wished to further explore the role of lipids on Alg2 activity. The enhancement of Alg2 enzyme activity was likely due to the presence of lipids rather than proteins because the membrane fraction added to the Alg2 reaction was denatured by heating at 100°C for 3 min (Fig. 1*A*). To test this idea, and to investigate what type of lipid contributes to increased Alg2 activity, we prepared proteoliposomes consisting of purified Trx-scAlg2 and different phospholipids, including PE, PS, CL, and PC. The choice of these lipids allowed a comparison of negatively charged (PS and CL) or neutral lipids (PE and PC) that also display different tendencies to form bilayers (PS and PC) or nonbilayer micelles (PE and CL) (22). The results of this experiment demonstrated a clear hierarchy of lipid effects (**Fig. 2**), with PC > >PE > >>>PS = CL. Proteoliposomes consisting of purified Alg2 and PC converted Man_1Gn_2-PPhy to Man_3Gn_2-PPhy efficiently (81% product at reaction

product are indicated by arrows. *C*) ESI-MS of glycans released from phytanyl oligosaccharides. Eluates shown in (*A*) were analyzed. Mass spectra of eluate from 8.7 to 9.2 min of Man_1Gn_2-PPhy (top), 10.8 to 11.3 min of sucrose (middle), and 12.3 to 12.6 min of sucrose and membrane (bottom) are shown. *D*) Linkage analysis of oligosaccharide produced by Trx-scAlg2. Peak around 12.4 min shown in *A* (sucrose and membrane) was collected, digested with indicated α-mannosidases, and analyzed by LC-MS.

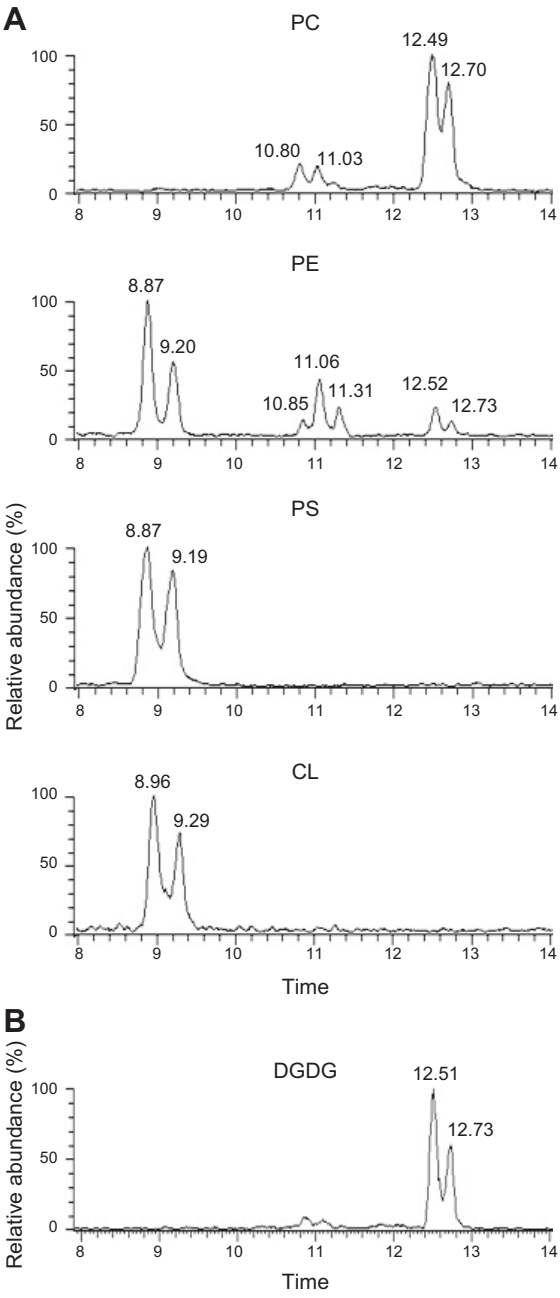

Figure 2. Effect of lipids on Trx-scAlg2 activity. Trx-scAlg2 proteoliposomes, consisting of pure protein and lipids, were prepared as described in Materials and Methods and used to assay MTase activity in standard reaction mixture. After 10 h incubation at 30°C, glycan released from reaction products were subjected to LC-MS analysis. Trx-scAlg2 proteoliposomes were prepared using following lipids: PE, PS, CL, PC. *B*) Trx-scAlg2 proteoliposomes were prepared with DGDG.

time of 10 h), while PS- or CL-containing proteoliposomes were inactive (Fig. 2*A*). PE-mixed proteoliposomes converted 13% of substrate to Man_3Gn_2 (Fig. 2*A*). One interpretation of these results is scAlg2 prefers zwitterionic-bilayer–prone lipid for its enzyme activity. To test this idea, another neutral bilayer lipid, DGDG, was tested. Alg2 activity in DGDG proteoliposomes was strongly enhanced (92% conversion of Man_1Gn_2-PPhy to Man_3Gn_2-PPhy) (Fig. 2*B*), supporting the idea that bilayer formation by net neutral lipids is critical for scAlg2 *in vitro* activity.

Trx-scAlg2 can directly transfer α1,6-linked Man to Man_1Gn_2-PPhy

To analyze the kinetics of the Alg2 reaction, we performed a time course, in which aliquots were removed at various times and analyzed by UPLC to measure short-lived reaction intermediates (**Fig. 3*A***). Interestingly, these intermediates were separated by UPLC into 3 distinct peaks around 11.0 min (Fig. 3*A*). In contrast, only a single intermediate peak was identified by ESI-MS, which corresponded to $[Gn_2\text{-}M_2 + Na]^+$ (Fig. 1*B*). These results suggested the possibility that this ESI-MS Man_2Gn_2 intermediate represents 2 isoforms, in which an α1,3- or α1,6-linked Man is attached at the nonreducing end of the Man_1Gn_2 substrate. To test this, we determined the linkage of the added Man. UPLC fractions containing intermediates were collected and treated with α1,2-3-mannosidase and α1,6-mannosidase. As shown in Fig. 3*B*, although these peaks were partially sensitive to either of these mannosidases, simultaneous treatment with both mannosidases resulted in their complete conversion to Man_1Gn_2 trisaccharide. In the tetrasaccharide mixture, the 10.64 and 10.93 min peaks that were the product of α1,2-3-mannosidase treatment originated from the Man-(α1,6)-Man_1Gn_2-PPhy (Fig. 3*B*, α1,2-3-mannosidase), while the 10.90 min and 11.14 min eluted peaks originated from the Man-(α1,3)-Man_1Gn_2-PPhy because it is the product of α1,6-mannosidase (Fig. 3*B*, third row). These results demonstrated that the intermediates identified by UPLC are a mixture of tetrasaccharides derived from Man-(α1,3)-Man_1Gn_2-PPhy and Man-(α1,6)-Man_1Gn_2-PPhy.

To further analyze the structure of the tetrasaccharide eluted from 10.6 to 11.0 min (Fig. 3*B*, second row), these two peaks were collected (Fig. 3*C*, *left*) and further treated with α1,6-mannosidase. This treatment resulted in complete conversion of this tetrasaccharide to Man_1Gn_2 (Fig. 3*C*, *right*), demonstrating the presence of Man-(α1,6)-Man_1Gn_2 in the intermediate mixture. Quantifying the area of the peaks revealed, after 2 h, 85% of the tetrasaccharide mixture was generated from Man-(α1,3)-Man_1Gn_2-PPhy and only 15% was from the Man-(α1,6)-Man_1Gn_2-PPhy. One interpretation of these data is that Trx-scAlg2 preferentially attached α1,3-linked Man to Man_1Gn_2-PPhy, followed by α1,6-linked Man to generate the final product Man-(α1,3)[Man-(α1,6)]-Man_1Gn_2-PPhy. These results are consistent with previous reports (11, 12). Importantly, the existence of the Man-(α1,6)-Man_1Gn_2-PPhy intermediate unequivocally demonstrated Trx-scAlg2 can directly attach an α1,6-linked Man to Man_1Gn_2-PPhy, which is then followed by α1,3-mannosylation to yield Man_3Gn_2-PPhy.

EX_7E, *N*-terminal cytosolic tail, and G-rich motif are required for Alg2 mannosyltransferase activity

To investigate amino acids predicted to be required for Alg2 function, we performed site-directed mutagenesis,

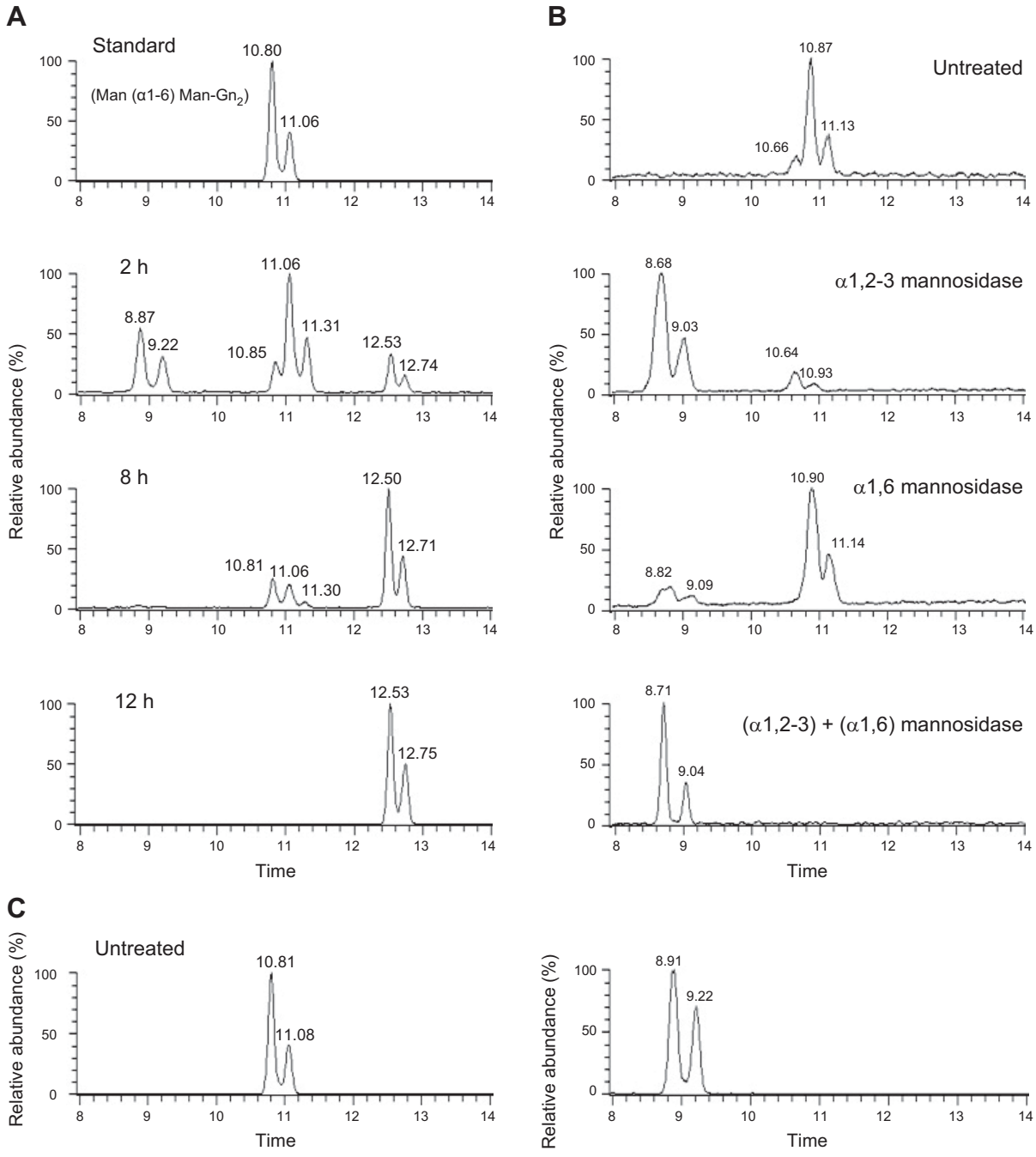

Figure 3. Linkage analysis of Trx-scAlg2 intermediates. *A*) Time-dependent formation of oligosaccharide intermediates. Reaction was performed under standard conditions over 12 h. Aliquots of reaction mixtures were removed at indicated times and analyzed by LC-MS. As standard, tetrasaccharide Man-(α1,6)-Man-Gn_2 was prepared by α1,2-3-mannosidase digestion of pentasaccharide Man-(α1,3)[Man-(α1,6)]-Man-Gn_2, which was formed on phytanyl group by Trx-scAlg2 activity. *B*) Linkage analysis of tetrasaccharide intermediates. Tetrasaccharide mixtures from each time point shown in *A* (2 h) were collected and digested with linkage-specific α-mannosidases. *C*) Tetrasaccharide eluted from 10.6 to 11.0 min in second row of *B*; these two peaks were accumulated and further treated with α1,6-mannosidase.

the effects of which were evaluated *in vitro* and *in vivo*. Most retaining GTases have a conserved EX_7E signature motif, whose role in catalysis as a nucleophile that stabilizes the donor substrate has been proposed (23, 24). Alg2 has an EX_7E motif in its C-terminal domain, but there are conflicting data about its importance. Kämpf *et al.* (12) reported the EX_7E motif was not required for Alg2 GTase function, while O'Reilly *et al.* (11) reported the conserved EX_7E motif is crucial. The importance of the Alg2 EX_7E motif was tested by altering each of the conserved Glu residues (E335 or E343 in the scAlg2 protein) or the H336 and F337 in the intervening X7 region to alanines (Fig. 4*A*). Each of these Trx-tagged mutant Alg2 proteins was expressed and purified from *E. coli*, and their activity measured using our MS-based *in vitro* assay (Fig. 1). For each reaction, the relative percentage of oligosaccharide

precursor, intermediate, and final product remaining after completion was determined (**Table 2**). The result of this experiment demonstrated that all these residues were important to varying degrees. Trx-scAlg2^{E335A}, mutated in the first E, had significantly decreased activity, producing no final product and only 32% of intermediate Man_2Gn_2 (Fig 4*B* and Table 2). Trx-scAlg2^{E343A}, mutated in the second E, had no detectable activity (Fig. 4*B* and Table 2). The intervening amino acids of the EX_7E were also important, though less than either E335 or E343. Trx-scAlg2^{H336A} and Trx-scAlg2^{F337A} produced 8% and 26% Man_3Gn_2 product, respectively (Fig. 4*B* and Table 2). Together, these results are in agreement with O'Reilly *et al.* and provide strong evidence that the EX_7E motif is important for Alg2 MTase activities *in vitro*.

Each mutation was also analyzed *in vivo* by measuring complementation of the *ALG2* deletion. Cells deleted for *ALG2* are inviable, so we used a plasmid shuffling technique to measure complementation (25). A yeast strain deleted for chromosomal *ALG2* (LST2) but that is kept alive by *ALG2* on a *URA3*-marked plasmid was constructed (see Materials and Methods). Each EX_7E *alg2*

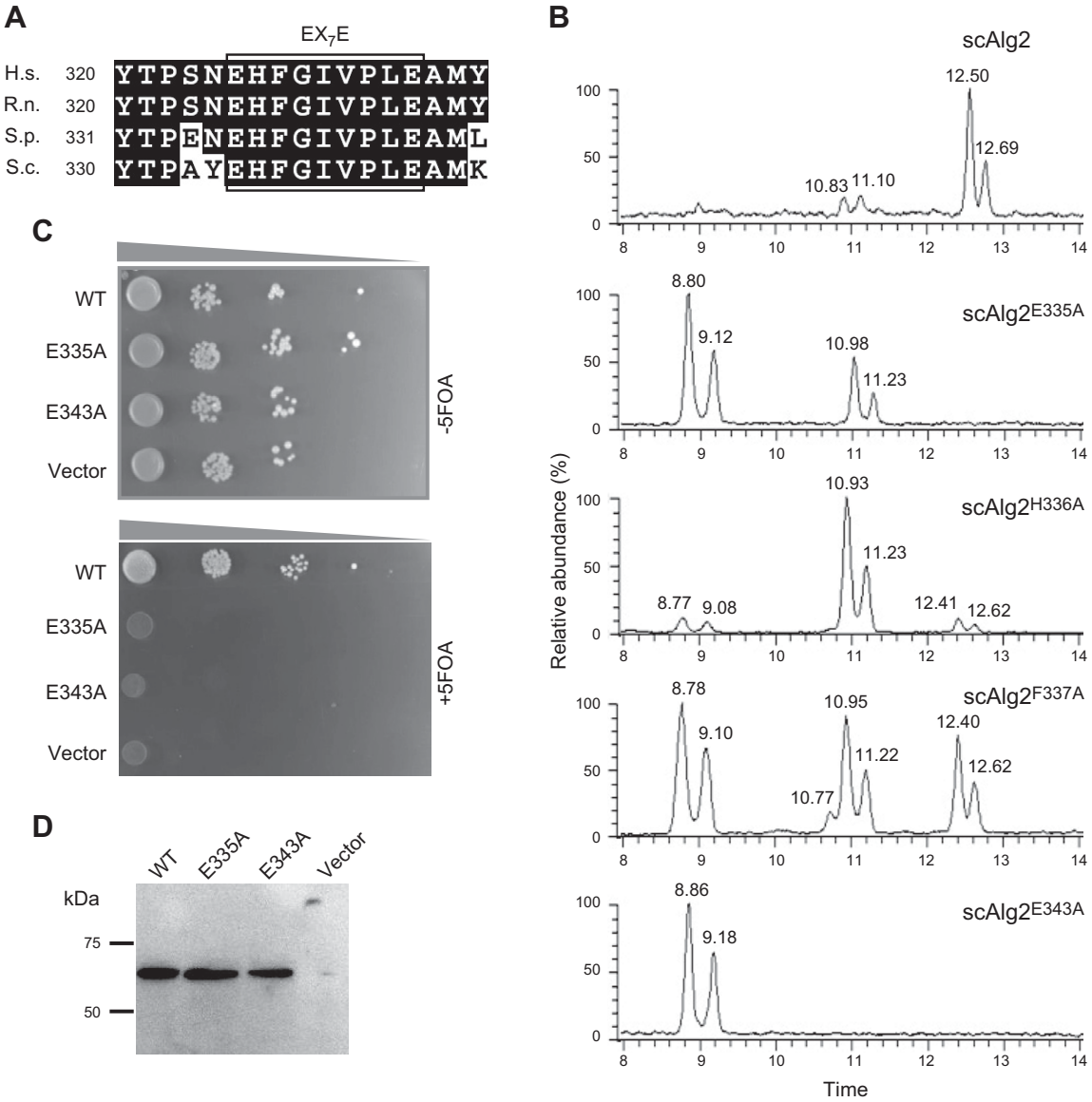

Figure 4. Site-directed mutagenesis of conserved EX_7E motif. *A*) Sequence alignment of Alg2 of *Homo sapiens* (H.s.), *Rattus norvegicus* (R.n.), *Schizosaccharomyces pombe* (S.p.), and *S. cerevisiae* (S.c.). Conserved EX_7E motif is marked in dark boxes. *B*) *In vitro* MTase activities of Trx-scAlg2 EX_7E mutants. Trx-scAlg2 proteins (mutant or WT) were expressed and purified from *E. coli.* Reactions were performed at 30°C for 10 h under standard conditions as described in Materials and Methods. Released glycans were subjected to LC-MS. *C*) Growth phenotypes of LSY2 strains harboring *TRP1*-marked plasmids, pRS314-3HA-scALG2 (WT), pRS314-3HA-scALG2^{E335A} (E335A), pRS314-3HA-scALG2^{E343A} (E343A), or pRS314-3HA (vector). Serial dilutions of strains expressing these plasmids were spotted on plates that contained uracil and 5-FOA but lacked tryptophan. As control, these strains were also spotted on plates lacking 5-FOA. Only cells expressing active Alg2 from *TRP1*-marked plasmid are able to grow on 5-FOA medium. Plates were incubated at 30°C for 48 h. *D*) Western blot analysis of scAlg2 proteins from *S. cerevisiae.* Membrane fractions of strains expressing each *alg2* allele were prepared as described in Materials and Methods. Equal amounts of proteins were analyzed by Western blot using anti-HA antibody.

TABLE 2. *Relative percentage of oligosaccharide produced by various Alg2 mutant proteins*[a]

WT/mutants	Conservation/motif	Man_1-Gn_2 (%)	Man_2-Gn_2 (%)	Man_3-Gn_2 (%)
WT	—	0	5	95
V62G	C	30	45	25
G17P	G rich	22	68 (α1,3)[b]	10
G19P	G rich	100	0	0
G20P	G rich	100	0	0
G256P	G rich	100	0	0
G257P	G rich	34	66 (α1,3)	0
E335A	EX_7E	68	32 (α1,3)	0
H336A	EX_7E	12	80 (α1,3)	8
F337A	EX_7E	40	34	26
E343A	EX_7E	100	0	0
G357P	G rich	100	0	0
G358P	G rich	95	5	0

Reactions were performed using purified WT or mutant Trx-scAlg2, GDP-Man, and Man_1Gn_2-PPhy. After incubation at 30°C for 10 h, glycans released from phytanyl anchor were subjected to LC-MS analysis. [a]Relative percentage of oligosaccharide was calculated using ratio of areas under oligosaccharide peak to total peak. Chromatograms of oligosaccharides that were produced by various mutant proteins are shown in Figs. 4*B*, 5*B*, and 6*B*. [b](α1,3) indicates mutants that catalyzed formation of Man-(α1,3)-Man_1Gn_2 isoform intermediate almost exclusively, as shown in Figs. 4*B* and 6*B*.

mutant allele (Fig. 4*A*) was introduced into this strain on a centromeric *TRP1*-marked plasmid. The rationale of this plasmid shuffling experiment is that *URA3* cells are inviable in the presence of 5-FOA so there is a strong selection for cells grown on 5-FOA to lose the *URA3* plasmid. Viable *ura3 alg2*Δ yeast can only grow on 5-FOA if the *TRP1*-marked plasmid-borne *alg2* mutant allele encodes a functional protein that can rescue the chromosomal *alg2*Δ deletion (25). To rule out dosage effects of *ALG2* overexpression, *TRP1*-marked expression of *alg2* mutant alleles was driven by the endogenous *ALG2* promoter in low-copy centromeric plasmids. Each *TRP1*-marked *alg2* allele was also tagged with HA to allow measurement of Alg2 protein levels by Western blot analysis. The results of these experiments demonstrated that both HA-scAlg2^{E335A} and HA-scAlg2^{E343A} mutants failed to support the growth of *alg2*Δ strain on 5-FOA plates (Fig. 4*C*), although their protein levels were indistinguishable from the WT HA-Alg2 (Fig. 4*D*). These results are in agreement with the experiments described above, and they demonstrate the importance of both E335 and E343 of the EX_7E domain for Alg2 function *in vivo* (Fig. 4*B*). Interestingly, we also found that Trx-scAlg2^{E335A} and Trx-scAlg2^{H336A} produced mainly the Man-(α1,3)-Man_1Gn_2 isoform intermediate, a result that was confirmed by UPLC (Fig. 4*B*) and α1,2,3-mannosidase treatment (data not shown). Thus, the second conserved E residue (E343) in the EX_7E motif of Alg2 is critical for both α1,3- and α1,6-mannosylations, while the first E (E335) and His-336 are partially required for α1,6-mannosylation.

These results are in conflict with those described by Kämpf *et al.* (12) and therefore raised the question of how they can be reconciled. We considered the possibility that the different activities observed by the same *alg2* EX_7E mutations could be explained by the different strain backgrounds used in these experiments, or by the possibility that Alg2 functions as an oligomer. All our *in vivo* complementation analyses were performed in a strain containing a complete deletion of *ALG2*, while Kämpf *et al.* used a temperature-sensitive *alg2-1* mutant containing a single missense mutation (G377R). If Alg2 were to form homodimers, then coexpression of two different *alg2* mutant alleles could result in intraallelic complementation. Although different nonfunctional *alg2* alleles encode a defective product when individually expressed, when coexpressed, they may encode polypeptides that physically interact, and this physical interaction could restore activity. Indeed, intraallelic complementation is a genetic hallmark of protein–protein interactions (26, 27). If this idea were correct, then Alg2 mutant homodimers would be inactive while Alg2 mutant heterodimers would be active.

To test this, we constructed *E. coli* strains that expressed the Trx-tagged *scalg2-1* (G377R) or *scalg2* E343A. Membrane fractions were prepared from these *E. coli* strains and Alg2 activity measured using our MS-based *in vitro* assay. As shown in Fig. 5, this experiment demonstrated that neither Alg2 [G377R (M)] nor E343A (M) membrane fractions displayed any mannosyltransferase activity, while 15% of activity was observed in membrane fractions from a mixture of Alg2 [G377R (M)] and E343A (M). These data provided strong evidence that these *alg2* alleles display intraallelic complementation and that these genetic interactions can explain the contradictory interpretations concerning the Alg2 EX_7E motif.

The *N*-terminal region of scAlg2, including 158 aa, containing both transmembrane domains as well as the short cytosolic tail was reported to be dispensable for Alg2 function because a deletion mutant lacking this domain could complement the temperature sensitivity of the yeast *alg2-1* mutant (12). This was surprising because a V68G substitution in the short *N*-terminus of human Alg2 underlies congenital myasthenic syndrome in humans, and this valine is highly conserved from yeast to human (Fig. 6*A*) (28). To test its importance, this V > G mutation was introduced at the corresponding position in scAlg2 (V62G). The recombinant Trx-scAlg2^{V62G} was purified from *E. coli* and its activity assayed *in vitro*. As shown in

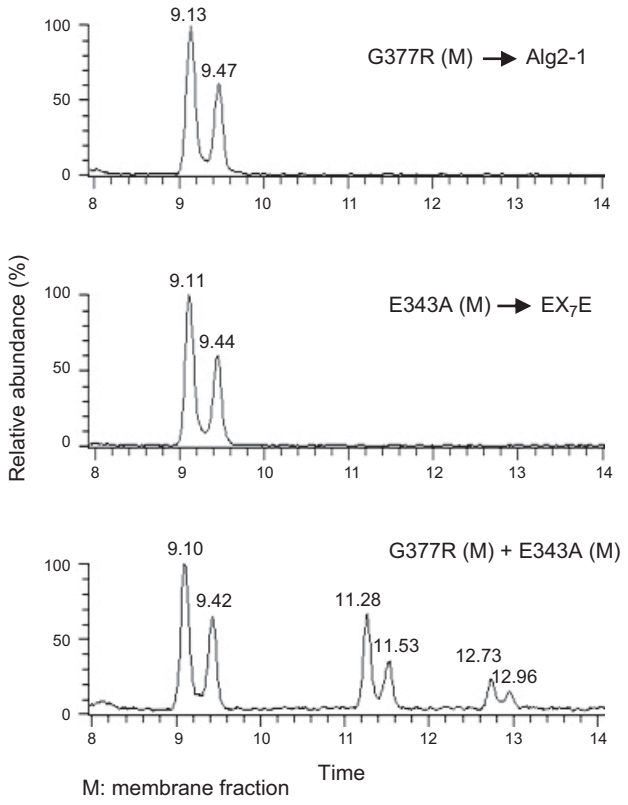

Figure 5. *In vitro* intraallelic complementation of scAlg2 mutants (*scalg2-1* G377R and *scalg2* E343A). Membrane fractions were prepared from *E. coli* expressing *scalg2-1* G377R and *scalg2* E343A as described in Materials and Methods. Reactions were performed using mutant membrane fractions G377R (M), E343A (M), or mixture of these membranes [(G377R (M)] + [E343A (M)] at 30°C for 10 h under standard reaction conditions as described in Materials and Methods. Glycans from oligosaccharide phytanyl products were released and subjected to LC-MS.

Fig. 6*B* and Table 2, this mutation severely affected Alg2 activity, producing ~25% of Man_3Gn_2 compared to WT Alg2. In addition, the HA-tagged mutant allele (3HA-scAlg2^{V62G}) failed to complement the lethality of the *alg2*Δ LSY2 when grown on 5-FOA (Fig. 6*C*), implying that, as in humans, the conserved Val residue is required for yeast Alg2 function.

This conserved V62 lies within a short cytosolic tail of scAlg2 (Fig. 6*A* and Supplemental Fig. S1). To test if this region is important for Alg2 function, *in vitro* and *in vivo* activity assays of mutant Alg2 lacking this *N*-terminal 65 aa were performed. Recombinant Trx-scAlg2$^{66–503}$ purified from *E. coli* was completely inactive *in vitro* (Fig. 6*B*), and this mutant allele also failed to complement LSY2 when grown on 5-FOA (Fig. 6*C*). However, in this case, the Alg2$^{66–503}$ protein could not be detected in yeast lysates by Western blot analysis (Fig. 6*D*). This experiment suggested that the failure of *alg2*$^{66–503}$ to complement growth on 5-FOA was due to Alg2 protein instability in yeast. These results suggested that the cytosolic *N*-terminal cytosolic tail is required for correct folding and/or stability of scAlg2.

G-rich motifs are hypothesized to function as flexible loops that are required for the conformational transitions during catalysis of many GTases (29). We identified three conserved G-rich motifs in scAlg2, located in the *N*-terminal cytosolic short tail, in the middle of Alg2, and in the C-terminal domain (**Fig. 7*A***and Supplemental Fig. S1). Each of these glycines, including G17, G19, G20, G256, G257, G357, and G358, was changed to proline and analyzed *in vitro* as described above. Each of these Trx-tagged mutant Alg2 proteins was expressed at similar level and purified from *E. coli* (data not shown). This experiment revealed that mutations in five of these glycines (G19, G20, G256, G357, G358) resulted in complete loss of activity, while two of them (G17, G257) were significantly decreased; scAlg2^{G17P} converted 10% of substrate to Man_3Gn_2 LLO, while scAlg2^{G257P} converted 66% of substrate into the intermediate Man_2Gn_2 (Fig. 7*B* and Table 2). Interestingly, scAlg2^{G17P} and scAlg2^{G257P} mainly produced a single isoform of intermediate, Man-(α1,3)-Man_1Gn_2, a conclusion based on UPLC retention times (Fig. 7*B*) and α1,2-3-mannosidase treatment (data not shown), indicating that these residues have critical contributions to α1,6-mannosylation. Notably, G17, G19, and G20 are within the *N*-terminal cytosolic tail of Alg2, further underscoring the importance of this domain for Alg2 function.

DISCUSSION

During the biosynthesis of LLO, Alg2 is responsible for the addition of both the α1,3- and α1,6-Man linkage onto Man_1Gn2-PDol to generate the trimannosyl core Man_3Gn_2-PDol. Although this bifunctionality has been recognized for some time, conflicting reports about the order of these reactions led to a gap in our understanding of these early events in LLO synthesis. In this study, we successfully developed an MS-based quantitative assay for Alg2 activity and applied it to study the enzyme activity of Alg2. This assay allowed us to precisely identify Alg2 reaction intermediates, demonstrating differentially linked Man can be added in either order, as well as amino acids that are required for Alg2 function *in vivo* and *in vitro*.

A requirement of *E. coli*–derived membranes for recombinant Trx-scAlg2 activity has been reported (11), but the contribution of native bacterial enzymes that copurified in those membrane fractions could not be ruled out (12). Using proteoliposomes reconstituted from pure phospholipids and recombinant Alg2, we demonstrated the lipids themselves are required for MTase activity (Fig. 2). Of the 5 lipids we tested, only PC and DGDG efficiently enhanced Alg2 activity (Fig. 2*A*). PC and DGDG are charge net-neutral lipids that have a propensity to form bilayers, and we speculate that these two characteristics are key for enhancing Alg2 activity (Fig. 2*B*). Many integral membrane proteins are affected by the lipid that surrounds them because lipid bilayers provide a hydrophobic thickness that matches that of hydrophobic transmembrane domain (30–34). On other hand, the charge balance rule proposes that net-neutral lipids like PC and DGDG can balance the charged transmembrane helix ends to dampen the potential of negatively charged residues (30, 33, 35, 36). scAlg2 has 2 *N*-terminal transmembrane helices flanked by many charged residues as well as two

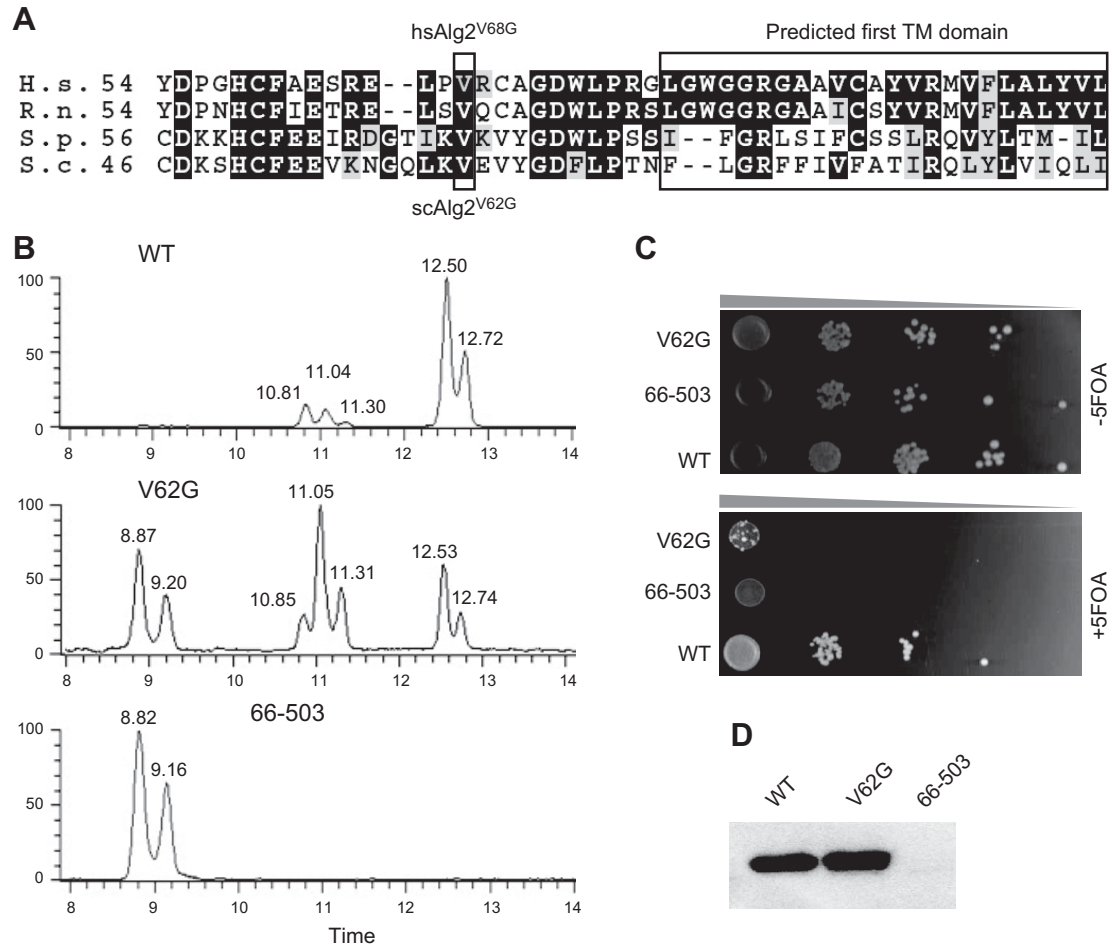

Figure 6. Site-directed mutagenesis of short *N*-terminal cytosolic tail of scAlg2. *A*) Alignment of *N*-terminus of Alg2 from *H. sapiens* (H.s.), *Danio rerio* (D.r.), *S. pombe* (S.p.), and *S. cerevisiae* (S.c.). Location of first predicted transmembrane domain as well as conserved V62 of *S. cerevisiae*, which corresponds to human V68, is boxed. *B*) *In vitro* activity of Trx-scAlg2^{WT} (WT), Trx-scAlg2^{V62G} (V62G), and Trx-scAlg2$^{66–503}$. Reaction conditions were as in Fig. 4*B*. *C*) Growth phenotypes of strains. Experimental condition was as in Fig. 4*C*. *D*) Western blot of Alg2 from LSY2 strains harboring pRS314-3HA-scAlg2^{V62G} (V62G), pRS314-3HA-scAlg2$^{66–503}$ (lacking first 65 aa), or pRS314-3HA-scAlg2 (WT). HA-tagged scAlg2 proteins were detected with anti-HA antibody.

hydrophobic C-terminal regions that associate with but do not cross the endoplasmic reticulum (Supplemental Fig. S1) (12). Net-neutral bilayer lipids PC and DGDG are likely to be necessary to create a bilayer thickness and ionic balance that is optimal for yeast Alg2 topology and function *in vitro*. In contrast to yeast Alg2, lipids are not required for the *in vitro* activity of purified human Alg2 (37). Human Alg2 contains only a single transmembrane domain at its *N*-terminus (37), so one explanation for the different lipid dependencies of yeast and human Alg2 may stem from their different membrane topologies.

A controversial issue we addressed in this study concerned the role of the conserved C-terminal EX$_7$E motif in Alg2 function. This motif is crucial for activity in those GTases so far examined (23, 24, 38–42). As expected from its evolutionary conservation, our mutational analyses demonstrated that both glutamic acids (E335 and E343) of the EX$_7$E, as well as residues in the intervening ×7 positions, are critical for scAlg2 function both *in vitro* and *in vivo* (Fig. 4). A likely explanation for the contradictions in the literature pertaining to the EX$_7$E is our observation that certain *alg2* mutations display intraallelic complementation *in vitro*. This was demonstrated by assaying the activity of individual mutant Alg2 proteins or a mixture of these proteins. By this assay, mutant Alg2 hetero-oligomers but not homo-oligomers were active. The mutant *alg2* alleles we assayed corresponded to the *alg2-1* allele used in previous complementation studies, therefore suggesting that EX$_7$E *alg2* mutants can complement *alg2-1 in vivo* through interallelic interactions, as we found *in vitro*. Our studies also implicate the *N*-terminal cytosolic tail (from 1 to 66 aa) as a critical determinant of Alg2 stability and thus MTase activity (Fig. 6). This result also disagrees with a previous study that reported the dispensability of *N*-terminal region (from 1 to 158 aa including the both transmembrane domains) for Alg2 *in vivo* (12). The effect of interallelic interactions described above may also provide an explanation for this contradiction. These results underscore a cautionary note for *in vivo* mutational analyses of genes that encode multimeric proteins and the necessity of performing complementation analyses in null mutant backgrounds.

One of the most interesting and unique aspects of Alg2 is its ability to catalyze two different reactions: addition of

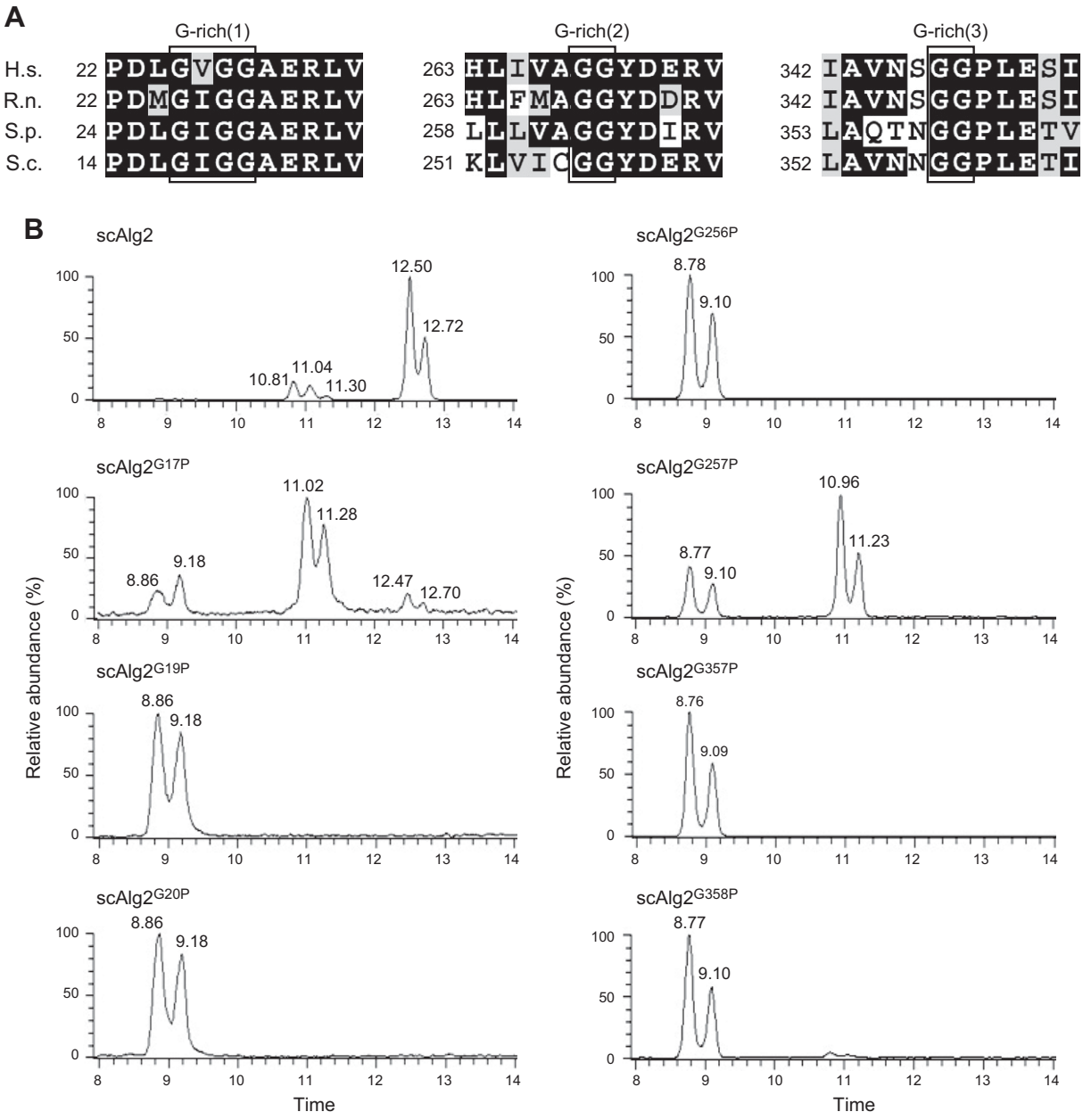

Figure 7. Site-directed mutagenesis of 3 conserved G-rich motifs. *A*) Sequence alignment of Alg2 of *H. sapiens* (H.s.), *R. norvegicus* (R.n.), *S. pombe* (S.p.), and *S. cerevisiae* (S.c.). Three conserved G-rich motifs are boxed. *B*) *In vitro* MTase activities of Trx-scAlg2 G-rich mutants. Reaction conditions were as in Fig. 4*B*.

both the α1,3- and α1,6-linked Man. An important and novel finding in this study is that these 2 reactions can occur independently of one another and in either order, albeit with different kinetics (Fig. 3). This finding was made possible by the high sensitivity of ESI-MS, which allowed the separation of mixed Man_2Gn_2-PPhy tetrasaccharide intermediates from one another as well as unambiguous confirmation of their structures with mannosidases (Fig. 3*C*). Recent studies reported no evidence for the existence of Man-(α1,6)-Man_1Gn_2 and therefore proposed a model for the Alg2 reaction in which formation of Man-(α1,3)-Man_1Gn_2-PPhy is a prerequisite for α1,6-linked Man addition (11, 12). We propose a different model, in which alternative orders of Man addition are possible. The α1,3-linked Man can be added first, followed by α1,6-linked Man or *vice versa* (**Fig. 8**, step 1→2 or step 3→4). By measuring the kinetics of oligosaccharide intermediate formation, we found Alg2 prefers to transfer the α1,3-linked Man to Man_1Gn_2-PPhy at early times because Man-(α1,3)-Man_1Gn_2-PPhy accumulated to higher levels (~80%) than Man-(α1,6)-Man_1Gn_2-PPhy (Fig. 3*A*, column of 2 h) (Fig. 8, step 1). At later times, almost all of the Man-(α1,3)-Man_1Gn_2-PPhy is converted to Man-(α1,6)[Man-(α1,3)]-Man_1Gn_2-PPhy, while most of the Man-(α1,6)-Man_1Gn_2-PPhy remains unmodified (Fig. 3*A*, column of 8 h). This suggests scAlg2 prefers to transfer the α1,6-linked Man to Man-(α1,3)-Man_1Gn_2-PPhy (Fig. 8, step 2) rather than the α1,3-linked Man to Man-(α1,6)-Man_1Gn_2-PPhy (Fig. 8, step 4). This appears to be a general rule, as yeast and human Alg2 behaved similarly (data not

shown). Thus, the major route of Alg2 is the transfer of α1,3-linked Man followed by α1,6-linked Man (Fig. 8, step 1→2).

The seemingly minor Alg2-mediated mannosylation route of glycosylation (Fig. 8, step 3→4) warrants attention because it occurs *in vivo* (8, 13) and, as we show here, *in vitro*. It is tempting to speculate that this minor route is a means by which cells can regulate flux through the LLO synthesis pathway. Studies by Harada *et al.* (43) provide indirect evidence for this idea. It has been known for some time that a low-glucose environment can arrest LLO biosynthesis. Harada *et al.* found that low-glucose–induced arrest of LLO biosynthesis results in substantial reductions of GDP-Man, which in turn leads to release of singly phosphorylated oligosaccharides into the cytosol. The most abundant cytosolic phosphorylated oligosaccharide is $Man_2GlcNAc_2$-P, leading to the hypothesis that the reaction depicted in Fig. 8, step 2 has a higher K_m for GDP-Man than step 1 in order to regulate the *N*-glycosylation state of the cell (43). In agreement with this idea, our results demonstrate the accumulation of the Man-(α1,3)-Man_1Gn_2-PPhy during early stages of the Alg2 reaction, which implies the rate of step 2 is slower than step 1 (Fig. 3*A*). This raises the interesting possibility that Alg2 may regulate LLO biosynthesis through the rate-limiting activity of step 2. It will be of interest to test this hypothesis by further biochemical studies of Alg2 that measure the K_m for GDP-Man of each step.

An important unanswered question is whether or not the dual Alg2 catalytic activities are distinct or share the same active site. For several reasons, we favor the idea that addition of both α1,3- and α1,6-linked Man are catalyzed *via* the same catalytic site. First, most bifunctional GTases are large (about 100 kDa) and contain two distinct, recognizable catalytic domains (44–47). In contrast, Alg2 is a small protein (503 aa) whose predicted catalytic domain is a GT-B fold. This fold consists of 2 Rossmann-like domains that face each other, with the catalytic site residing in the cleft between them (48). In addition, for bifunctional GTases with two separate domains, site-directed mutagenesis of residues in each domain specifically affect the corresponding sugar addition (44–46). Mutation of numerous Alg2 residues throughout its length has failed to identify any that specifically affect α1,3-linked Man additions, implying that both of α1,3- and α1,6-linked Man additions are catalyzed *via* the same catalytic site.

If Alg2 has a single catalytic site, how can it carry out catalysis of two different linkages? Structural analyses of several GTase implicate one or two flexible G-rich loops at the substrate binding site that undergo a marked conformational transition upon donor binding (29, 34, 49–51). We hypothesize that Alg2 catalyzes Man_1Gn_2-PDol to Man_3Gn_2-PDol through sequential conformation transitions that involve G-rich flexible loops at Gly17 and Gly257. These residues are highly conserved and critical for α1,6-mannosylation of Man-(α1,3)-Man_1Gn_2-PDol (Fig. 8, step 2; Fig. 7*B*). One hypothesis is when Alg2 transfers the α1,3-linked Man to Man_1Gn_2-PDol (Fig. 8, step 1), a conformational transition mediated by a G-rich loop alters the specificity required for subsequent transfer of α1,6-linked Man to Man-(α1,3)-Man_1Gn_2-PDol. Testing this hypothesis will require structural studies to define the conformational changes in Alg2 that are triggered by its various substrate interactions during α1,3- and α1,6-linked Man addition. Several mutations we identified, including $scAlg2^{H336A}$ (Fig. 4) and $scAlg2^{G257P}$ (Fig. 8),

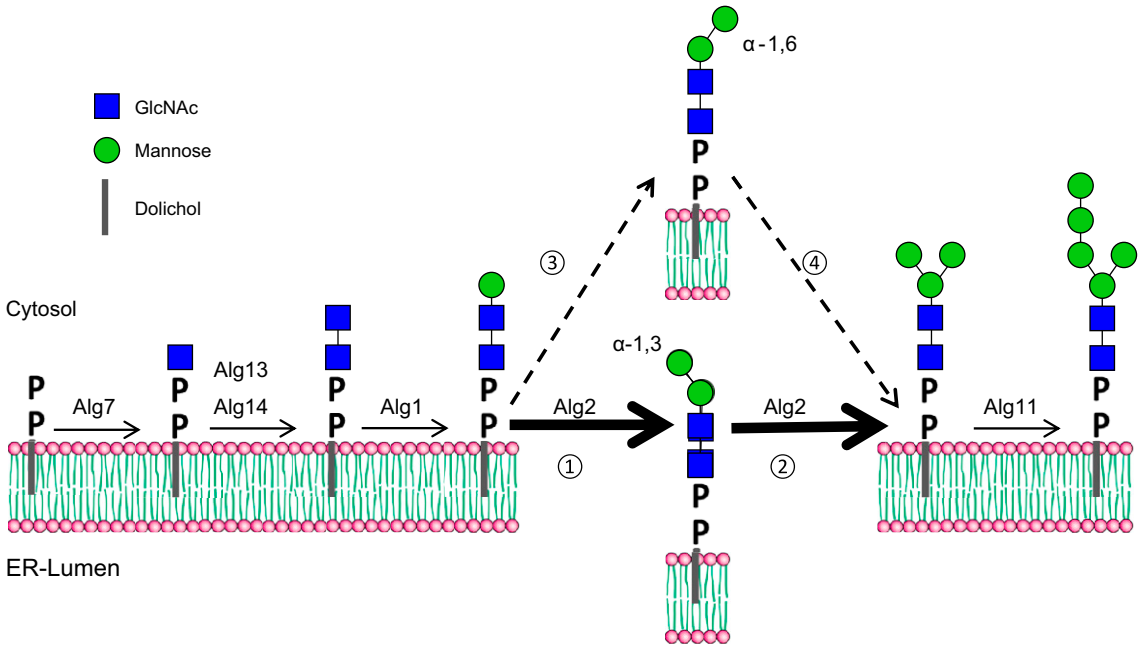

Figure 8. Proposed model of $Man_3GlcNAc_2$-PDol catalyzed by Alg2. Sequential reactions by Alg7, Alg13/14 heterooligomer, and Alg1 generate Alg2 substrate, $Man_1GlcNAc_2$-PDol (Man_1Gn_2-PDol). Dual activities of Alg2 allow transfer of Man to β1,4-linked Man of Man_1Gn_2-PDol with either α1,3 (reaction 1) or α1,6 linkage (reaction 3). Resulting linear tetrasaccharides are branched by Alg2-dependent mannosylations with α1,6 linkage (reaction 2) or α1,3 linkage (reaction 4), yielding $Man_3GlcNAc_2$-PDol (Man_3Gn_2-PDol) for further elongation by Alg11.

produce only Man-(α1,3)-Man_1Gn2-PPhy. These mutants, along with the *in vitro* system we described, suggest the feasibility of future cryoelectron microscopy studies using these mutants as an approach to capture these transient intermediate complexes. FJ

ACKNOWLEDGMENTS

This work was supported by grants-in-aid from the National Natural Science Foundation of China (21778023, 21576118, 31770853, 31400693), Natural Science Foundation of Jiangsu Province (BK20170174), Fundamental Research Funds for the Central Universities (JUSRP51629B, JUSRP11727), Program of Introducing Talents of Discipline to Universities (111-2-06), and Young Thousand Program (to M.F.). The authors declare no conflicts of interest.

AUTHOR CONTRIBUTIONS

S.-T. Li, N. Wang, X.-X. Xu, T. Kitajima, and X.-D. Gao performed experiments and analyzed data; M. Fujita and H. Nakanishi provided expertise and feedback; N. Dean and X.-D. Gao proposed and supervised the project and wrote the article; and all authors confirmed and edited the article.

REFERENCES

1. Aebi, M., Bernasconi, R., Clerc, S., and Molinari, M. (2010) *N*-glycan structures: recognition and processing in the ER. *Trends Biochem. Sci.* **35**, 74–82
2. Satoh, T., Yamaguchi, T., and Kato, K. (2015) Emerging structural insights into glycoprotein quality control coupled with *N*-glycan processing in the endoplasmic reticulum. *Molecules* **20**, 2475–2491
3. Schwarz, F., and Aebi, M. (2011) Mechanisms and principles of *N*-linked protein glycosylation. *Curr. Opin. Struct. Biol.* **21**, 576–582
4. Schmaltz, R. M., Hanson, S. R., and Wong, C. H. (2011) Enzymes in the synthesis of glycoconjugates. *Chem. Rev.* **111**, 4259–4307
5. Huffaker, T. C., and Robbins, P. W. (1983) Yeast mutants deficient in protein glycosylation. *Proc. Natl. Acad. Sci. USA* **80**, 7466–7470
6. Aebi, M. (2013) *N*-linked protein glycosylation in the ER. *Biochim. Biophys. Acta* **1833**, 2430–2437
7. Jackson, B. J., Kukuruzinska, M. A., and Robbins, P. (1993) Biosynthesis of asparagine-linked oligosaccharides in *Saccharomyces cerevisiae*: the *alg2* mutation. *Glycobiology* **3**, 357–364
8. Jackson, B. J., Warren, C. D., Bugge, B., and Robbins, P. W. (1989) Synthesis of lipid-linked oligosaccharides in *Saccharomyces cerevisiae*: $Man_2GlcNAc_2$ and $Man_1GlcNAc_2$ are transferred from dolichol to protein *in vivo*. *Arch. Biochem. Biophys.* **272**, 203–209
9. Takeuchi, K., Yamazaki, H., Shiraishi, N., Ohnishi, Y., Nishikawa, Y., and Horinouchi, S. (1999) Characterization of an *alg2* mutant of the zygomycete fungus *Rhizomucor pusillus*. *Glycobiology* **9**, 1287–1293
10. Thiel, C., Schwarz, M., Peng, J., Grzmil, M., Hasilik, M., Braulke, T., Kohlschütter, A., von Figura, K., Lehle, L., and Körner, C. (2003) A new type of congenital disorders of glycosylation (CDG-Ii) provides new insights into the early steps of dolichol-linked oligosaccharide biosynthesis. *J. Biol. Chem.* **278**, 22498–22505
11. O'Reilly, M. K., Zhang, G., and Imperiali, B. (2006) *In vitro* evidence for the dual function of Alg2 and Alg11: essential mannosyltransferases in *N*-linked glycoprotein biosynthesis. *Biochemistry* **45**, 9593–9603
12. Kämpf, M., Absmanner, B., Schwarz, M., and Lehle, L. (2009) Biochemical characterization and membrane topology of Alg2 from *Saccharomyces cerevisiae* as a bifunctional alpha1,3- and 1,6-mannosyltransferase involved in lipid-linked oligosaccharide biosynthesis. *J. Biol. Chem.* **284**, 11900–11912
13. Prakash, C., and Vijay, I. K. (1982) Characterization of intermediates up to lipid-linked heptasaccharide implicated in the biosynthesis of *Saccharomyces cerevisiae* mannoproteins. *Biochemistry* **21**, 4810–4818
14. Campbell, J. A., Davies, G. J., Bulone, V., and Henrissat, B. (1997) A classification of nucleotide-diphospho-sugar glycosyltransferases based on amino acid sequence similarities. *Biochem. J.* **326**, 929–939
15. Li, S. T., Wang, N., Xu, S., Yin, J., Nakanishi, H., Dean, N., and Gao, X. D. (2017) Quantitative study of yeast Alg1 beta-1, 4 mannosyltransferase activity, a key enzyme involved in protein *N*-glycosylation. *Biochim. Biophys. Acta* **1861** (1 Pt A), 2934–2941
16. Ho, S. N., Hunt, H. D., Horton, R. M., Pullen, J. K., and Pease, L. R. (1989) Site-directed mutagenesis by overlap extension using the polymerase chain reaction. *Gene* **77**, 51–59
17. Vitrac, H., Bogdanov, M., and Dowhan, W. (2013) Proper fatty acid composition rather than an ionizable lipid amine is required for full transport function of lactose permease from *Escherichia coli*. *J. Biol. Chem.* **288**, 5873–5885
18. Guthrie, C. (2002) *Guide to Yeast Genetics and Molecular and Cell Biology*, Academic Press, New York
19. Longtine, M. S., Mckenzie Iii, A., Demarini, D. J., Shah, N. G., Wach, A., Brachat, A., Philippsen, P., and Pringle, J. R. (1998) Additional modules for versatile and economical PCR-based gene deletion and modification in *Saccharomyces cerevisiae*. *Yeast* **14**, 953–961
20. Lu, J., Takahashi, T., Ohoka, A., Nakajima, K., Hashimoto, R., Miura, N., Tachikawa, H., and Gao, X. D. (2012) Alg14 organizes the formation of a multiglycosyltransferase complex involved in initiation of lipid-linked oligosaccharide biosynthesis. *Glycobiology* **22**, 504–516
21. Pabst, M., and Altmann, F. (2008) Influence of electrosorption, solvent, temperature, and ion polarity on the performance of LC-ESI-MS using graphitic carbon for acidic oligosaccharides. *Anal. Chem.* **80**, 7534–7542
22. Dowhan, W., and Bogdanov, M. (2012) Molecular genetic and biochemical approaches for defining lipid-dependent membrane protein folding. *Biochim. Biophys. Acta* **1818**, 1097–1107
23. Geremia, R. A., Petroni, E. A., Ielpi, L., and Henrissat, B. (1996) Towards a classification of glycosyltransferases based on amino acid sequence similarities: prokaryotic alpha-mannosyltransferases. *Biochem. J.* **318**, 133–138
24. Kapitonov, D., and Yu, R. K. (1999) Conserved domains of glycosyltransferases. *Glycobiology* **9**, 961–978
25. Boeke, J. D., Trueheart, J., Natsoulis, G., and Fink, G. R. (1987) 5-Fluoroorotic acid as a selective agent in yeast molecular genetics. *Methods Enzymol.* **154**, 164–175
26. Qureshi, A. A., Crane, A. M., Matiaszuk, N. V., Rezvani, I., Ledley, F. D., and Rosenblatt, D. S. (1994) Cloning and expression of mutations demonstrating intragenic complementation in mut0 methylmalonic aciduria. *J. Clin. Invest.* **93**, 1812–1819
27. Chirala, S. S., Kuziora, M. A., Spector, D. M., and Wakil, S. J. (1987) Complementation of mutations and nucleotide sequence of *FAS1* gene encoding beta subunit of yeast fatty acid synthase. *J. Biol. Chem.* **262**, 4231–4240
28. Cossins, J., Belaya, K., Hicks, D., Salih, M. A., Finlayson, S., Carboni, N., Liu, W. W., Maxwell, S., Zoltowska, K., Farsani, G. T., Laval, S., and Seidhamed, M. Z.; WGS500 Consortium. (2013) Congenital myasthenic syndromes due to mutations in *ALG2* and *ALG14*. *Brain* **136**, 944–956
29. Qasba, P. K., Ramakrishnan, B., and Boeggeman, E. (2005) Substrate-induced conformational changes in glycosyltransferases. *Trends Biochem. Sci.* **30**, 53–62
30. Dowhan, W., and Bogdanov, M. (2009) Lipid-dependent membrane protein topogenesis. *Annu. Rev. Biochem.* **78**, 515–540
31. Seelig, J. (2004) Thermodynamics of lipid–peptide interactions. *Biochim. Biophys. Acta* **1666**, 40–50
32. Tilley, S. J., Orlova, E. V., Gilbert, R. J. C., Andrew, P. W., and Saibil, H. R. (2005) Structural basis of pore formation by the bacterial toxin pneumolysin. *Cell* **121**, 247–256
33. Agasøster, A. V., Halskau, Ø., Fuglebakk, E., Frøystein, N. A., Muga, A., Holmsen, H., and Martínez, A. (2003) The interaction of peripheral proteins and membranes studied with alpha-lactalbumin and phospholipid bilayers of various compositions. *J. Biol. Chem.* **278**, 21790–21797
34. Giganti, D., Alegre-Cebollada, J., Urresti, S., Albesa-Jové, D., Rodrigo-Unzueta, A., Comino, N., Kachala, M., López-Fernández, S., Svergun, D. I., Fernández, J. M., and Guerin, M. E. (2013) Conformational plasticity of the essential membrane-associated mannosyltransferase PimA from mycobacteria. *J. Biol. Chem.* **288**, 29797–29808
35. Baenziger, J. E., Morris, M. L., Darsaut, T. E., and Ryan, S. E. (2000) Effect of membrane lipid composition on the conformational

equilibria of the nicotinic acetylcholine receptor. *J. Biol. Chem.* **275**, 777–784
36. Kirsch, T., Nah, H. D., Demuth, D. R., Harrison, G., Golub, E. E., Adams, S. L., and Pacifici, M. (1997) Annexin V–mediated calcium flux across membranes is dependent on the lipid composition: implications for cartilage mineralization. *Biochemistry* **36**, 3359–3367
37. Ramírez, A. S., Boilevin, J., Lin, C.-W., Ha Gan, B., Janser, D., Aebi, M., Darbre, T., Reymond, J.-L., and Locher, K. P. (2017) Chemoenzymatic synthesis of lipid-linked $GlcNAc_2Man_5$ oligosaccharides using recombinant Alg1, Alg2 and Alg11 proteins. *Glycobiology* **27**, 1–8
38. Cid, E., Gomis, R. R., Geremia, R. A., Guinovart, J. J., and Ferrer, J. C. (2000) Identification of two essential glutamic acid residues in glycogen synthase. *J. Biol. Chem.* **275**, 33614–33621
39. Abdian, P. L., Lellouch, A. C., Gautier, C., Ielpi, L., and Geremia, R. A. (2000) Identification of essential amino acids in the bacterial alpha-mannosyltransferase aceA. *J. Biol. Chem.* **275**, 40568–40575
40. Absmanner, B., Schmeiser, V., Kämpf, M., and Lehle, L. (2010) Biochemical characterization, membrane association and identification of amino acids essential for the function of Alg11 from *Saccharomyces cerevisiae*, an alpha1,2-mannosyltransferase catalysing two sequential glycosylation steps in the formation of the lipid-linked core oligosaccharide. *Biochem. J.* **426**, 205–217
41. Kostova, Z., Yan, B. C., Vainauskas, S., Schwartz, R., Menon, A. K., and Orlean, P. (2003) Comparative importance *in vivo* of conserved glutamate residues in the EX7E motif retaining glycosyltransferase Gpi3p, the UDP-GlcNAc–binding subunit of the first enzyme in glycosylphosphatidylinositol assembly. *Eur. J. Biochem.* **270**, 4507–4514
42. Huang, Y. C., Hsiang, E. C., Yang, C. C., and Wang, A. Y. (2016) New insight into the catalytic properties of rice sucrose synthase. *Plant Mol. Biol.* **90**, 127–135
43. Harada, Y., Nakajima, K., Masahara-Negishi, Y., Freeze, H. H., Angata, T., Taniguchi, N., and Suzuki, T. (2013) Metabolically programmed quality control system for dolichol-linked oligosaccharides. *Proc. Natl. Acad. Sci. U S A* **110**, 19366–19371
44. Jing, W., and DeAngelis, P. L. (2003) Analysis of the two active sites of the hyaluronan synthase and the chondroitin synthase of *Pasteurella multocida*. *Glycobiology* **13**, 661–671
45. Jing, W., and DeAngelis, P. L. (2000) Dissection of the two transferase activities of the *Pasteurella multocida* hyaluronan synthase: two active sites exist in one polypeptide. *Glycobiology* **10**, 883–889
46. Van Der Wel, H., Fisher, S. Z., and West, C. M. (2002) A bifunctional diglycosyltransferase forms the Fucalpha1,2Galbeta1,3-disaccharide on Skp1 in the cytoplasm of dictyostelium. *J. Biol. Chem.* **277**, 46527–46534
47. Hwang, H. Y., Olson, S. K., Esko, J. D., and Horvitz, H. R. (2003) *Caenorhabditis elegans* early embryogenesis and vulval morphogenesis require chondroitin biosynthesis. *Nature* **423**, 439–443
48. Albesa-Jové, D., Giganti, D., Jackson, M., Alzari, P. M., and Guerin, M. E. (2014) Structure–function relationships of membrane-associated GT-B glycosyltransferases. *Glycobiology* **24**, 108–124
49. Wu, R., Asención Diez, M. D., Figueroa, C. M., Machtey, M., Iglesias, A. A., Ballicora, M. A., and Liu, D. (2015) The crystal structure of nitrosomonas europaea sucrose synthase reveals critical conformational changes and insights into sucrose metabolism in prokaryotes. *J. Bacteriol.* **197**, 2734–2746
50. Breton, C., Snajdrová, L., Jeanneau, C., Koca, J., and Imberty, A. (2006) Structures and mechanisms of glycosyltransferases. *Glycobiology* **16**, 29R–37R
51. Sheng, F., Jia, X., Yep, A., Preiss, J., and Geiger, J. H. (2009) The crystal structures of the open and catalytically competent closed conformation of *Escherichia coli* glycogen synthase. *J. Biol. Chem.* **284**, 17796–17807

Received for publication November 6, 2017.
Accepted for publication December 5, 2017.

Alternative routes for synthesis of *N*-linked glycans by Alg2 mannosyltransferase

Sheng-Tao Li, Ning Wang, Xin-Xin Xu, et al.

FASEB J published online December 22, 2017
Access the most recent version at doi:10.1096/fj.201701267R

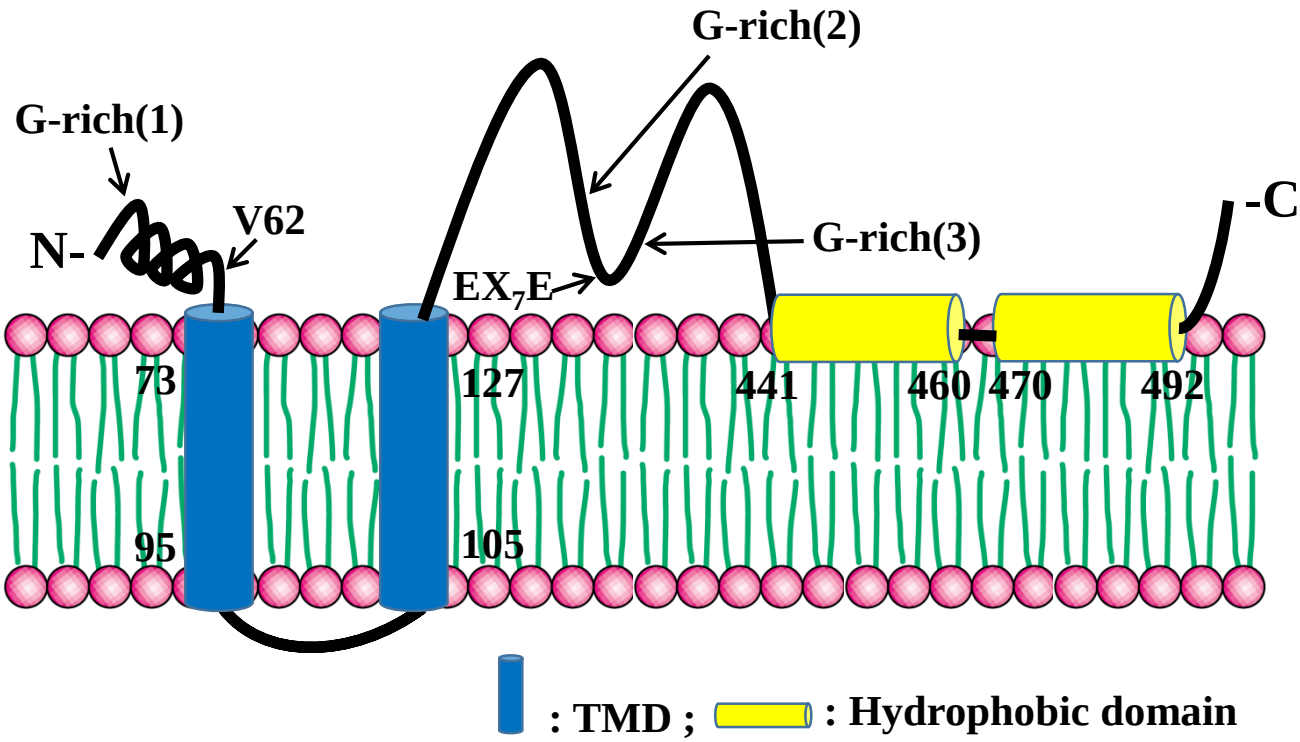

Supplemental fig. 1 Li et al.